Bulgarian Academy of Sciences. Space Research and Technology Institute.
Aerospace Research in Bulgaria. 26, 2014, Sofia

SOME AEROSPACE APPLICATIONS OF OPTICAL POLYMERS

Ivan Nikolov[1], Stefka Kasarova[2], Nina Sultanova[2]

[1]Sofia University, Faculty of Physics, Dept. of Optics and Spectroscopy
[2]University "Assen Zlatarov" – Bourgas, Dept. of Mathematics and Physics
e-mail: kasarova_st@yahoo.com

Abstract

Optical polymers (OPs) are widely used in optoelectronic stations intended for remote imaging diagnostics of Earth's surface. A number of new applications in aerospace technology of polymer materials such as hybrid and nanocomposite structures are pointed out. A multi-spectral camera for remote analysis of forest and agriculture areas is presented. Remote sensing spectrometer setups with a 3D hyper-spectral cube of the Earth's pictures are discussed. Image quality of optical elements is guaranteed on base of calculated geometrical and wave aberrations. An analysis for thermo-optical aberrations is fulfilled. An optimized video-spectrometer mirror-lens system intended for a SITe CCD sensor is explained.

Biomedical applications of OPs are included. It is pointed out that doctors control constantly the medical characteristics of eye vision and digestive tract of pilots before every flight. Polymer helmet and binocular displays, used by spacemen and aviators, are analyzed. A swallowable disposable capsule camera, made of OPs, and intended for remote biomedical examinations of the aviation staff is pictured.

1. Introduction

Imaging spectrometer systems present a new generation of equipment tools, intended for remote sensing (RS), of various natural objects located on the surface of the Earth and planets [1-14]. The essence of RS consists in obtaining the necessary information about the observed object by measuring its distance, as well as in processing of received remote data on energy and polarization characteristics of heat radiation emitted, reflected or scattered by Earth land- or ocean-surface and atmosphere in different regions of the electromagnetic spectrum. These radiance

measurements are used for environmental and defense applications, weather prediction, and global change studies. RS methods enable determination of objects' location and describe temporal dynamics of the major natural forms and phenomena of Earth resources [2, 15]. Some optical systems intended for remote research are examined in [3].

RS instruments and systems are widely used in the last decades for high-quality spectral radiation measurements from satellite-, aircraft-, and ground-based laboratories. [1, 2, 4, 6-14, 16]. Basic peculiarity of RS optical devices is their high information capacity for the transfer and processing of optical images. Data obtained from different ground swaths is detected by two-dimensional (2D) CCD matrices and recorded in the spectrometer. The created 2D optical image is scanned sequentially and registered in lines in different bands of the spectrum [6]. The video spectrophotometric information is downloaded in the memory of the optical device and forms the so called *Hyperspectral Cube.* The method involves acquisition of image data of the 2D photo in many contiguous spectral bands and monochromatic images from 310 to 900 are recorded. Information volume of a hyperspectral cube is about 10^9 bits for one pixel on the Earth surface. For one revolution around the Earth, the remote system can accumulate about 50-100 thousands of photos, and the volume of the optical memory exceeds 10^{12} bytes [3, 4, 6-14]. The objective of the video spectrometer Vega 2, which has been used for photographing and investigation of Halley's comet, is based on the optical scheme of Cassegrain [3, 17].

In Bulgarian Academy of Science, under the guidance of academician D. Mishev, multichannel spectrometric systems Spectrum-15 [2, 3] and Spectrum-256 [4] were constructed which have been used by the aircraft of Mir space station. The contemporary hybrid devices, widely applied in aerospace experiments, provide imaging of remote objects in all parts of the electromagnetic spectrum, including UV, VIS and NIR spectral bands, and accomplish spectral-zonal photometry of Earth surface [1-4, 6-8]. The recorded images are then subjected to optical and digital processing to obtain the maximum information about the investigated remote objects [3, 4]. However, wavelengths at which absorption of light by Earth atmosphere occurs are eliminated. This is a restriction for the applied optical instruments. It is important to emphasize that directly measured characteristics of the radiation field as brightness or intensity are functions of two types of independent variables [2]: 1) wavelength, field of view, zenith and azimuth angle of Sun, etc..; 2) parameters that depend on the

distribution of the basic physical characteristics of the atmosphere (air temperature, concentration of gas components, aerosols, and the like.). The obtained spectral images are particularly suitable for the study of characteristics and the dynamic status of plant sites, and also to create methods for determining the influence of different vegetation and stress factors.

Multi-spectral imaging in orbital stations of satellites Landsat and Spot is carried out within three to seven clear spectral regions. NASA satellites are the first spectrometers having high resolution for operation in space which take photographs of the Earth surface in 384 narrow bands for the spectral region from 400 to 2500 nm [6].

Unique properties of OPs as reduced weight and cost, high impact and shatter resistance, and ability to integrate proper mechanical and optical features make them preferred materials in the design of aerospace optic instruments and devices [18]. Most popular for this purpose are the acrylic based polymers, polycarbonates, cyclo olefin polymers and copolymers, polystyrenes, alicyclic methacrylate copolymers [5]. Obviously, unique priority of polymers for biomedical applications is safety. Some measured optical and material characteristics of OPs are reported. In this paper we also present the design of a remote imaging mirror-lens polymer system, based on the classical Cassegrain optical scheme, which is widely used in astronomy and space research. It is composed of a concave primary mirror and a convex central mirror, and the foci of both mirrors coincide [17]. Popular objectives consist of two spherical mirrors and aberration compensators [3].

2. Analysis of Video Spectrometers Optical Schemes

Principal optical scheme of an imaging spectrometer with a pushbroom approach to image acquisition is illustrated in Fig. 1a and for a linear scanning system - in Fig. 1b. Video spectrometer examines a photographed ground swath located perpendicular to the satellite motion. The spectral cube contains 384 color images with a detailed data about spectral signatures of objects in each pixel (Fig. 2: water, soil, grass). Remote sensing of Earth has a history: each of the agricultures and its vegetation is observed from space station using satellites and video spectrometers [1, 2, 4, 6]. Moreover, with the help of video spectroscopy it is possible to control the early detection of diseases in wheat and trees, the

location of minerals, fish migration and a number of similar processes at the Earth surface. Spectral image is a collection of images of one and the same

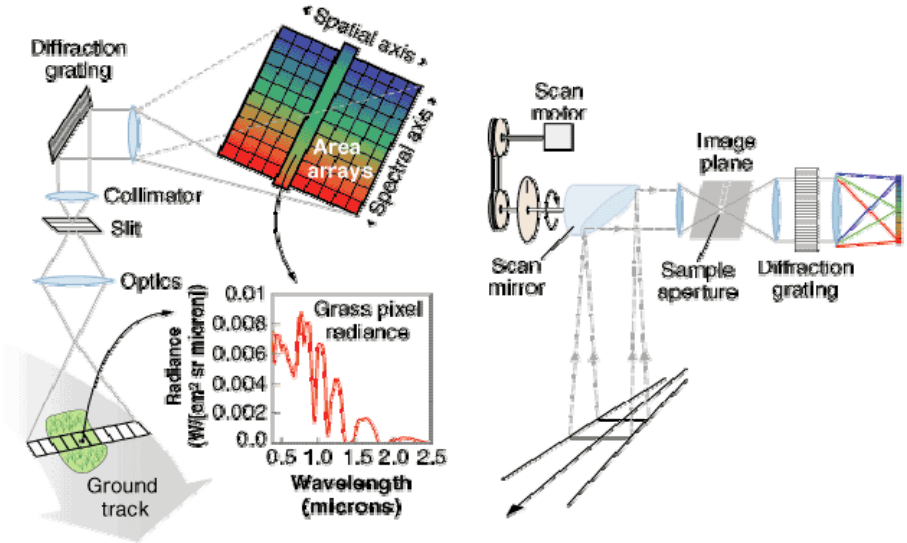

Fig. 1. Imaging Spectrometer Optical Setups: (a) a push-broom design; (b) a line-scanner device for reflection spectra

object in different parts of the spectrum (Fig. 2). The usual picture is two-dimensional with XY axes, but spectral images have a third dimension, i.e. spectral axis Z. This creates a spectral cube of each frame, where each copy of the image along the vertical axis Z is a set of images seen in colors at fixed wavelengths. Classical spectrometers collect measurement data in a single spectral curve and provide this information through a series of numbers or in graphical form. Video spectrometers generate full details for the whole investigated surface of the Earth object [4, 5-14]. Video spectrometer, type "Pushbroom", works mainly as a manual copier in space: the optical instrument rotates around the Earth and "is sweeping" information from all object points in its field of view (Fig. 1a). The technique "Whiskbroom" scans the area in the field of view of the device by scanning mirrors or specialized optics similarly in the way a TV set scans quickly the light beam on the screen (Fig. 1b).

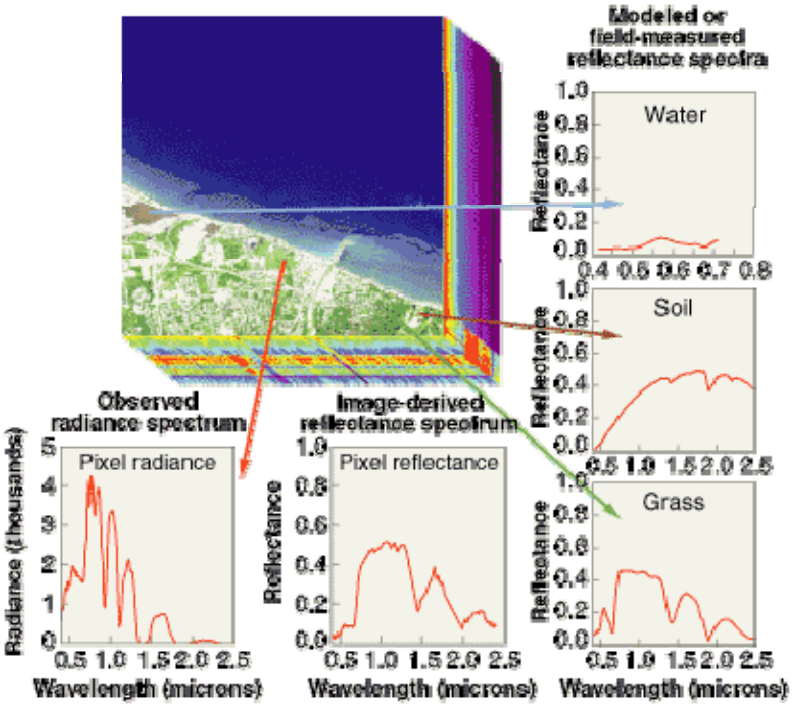

Fig. 2. Decoding of images of objects recorded by the video spectrometer in the hyperspectral cube: water, soil and grass

Video spectrometers are divided into the following major groups: multispectral (a number of groups), hyperspectral (several hundreds of groups) and ultraspectral (several thousands of groups). Each group provides progressively more information in the form of a dense aggregations of one image. Multispectral video spectrometers generally use the method of whiskbroom. Hyperspectral system applies pushbroom and whiskbroom setups in order to gain as much information as possible. Ultraspectral video spectrometers combine several instruments and both methods to gather the most detailed information [6-11]. Data processing of spectral luminance is used for a wide range of purposes such as: identification of minerals in rocks and soil, measured organic content, pollution of oceans and groundwater, etc. [15].

Remote imaging technologies provide registration of the absorption properties of geographic elements such as plant areas, rocks or urban areas. Multi-spectral imaging devices operate in 3 or 7 spectral bands (Fig. 3).

Hyper-spectral imaging devices photograph the surface of the Earth with high resolution in 384 narrow spectral bands in the range from 400 to 2500 nm [6, 7, 11]. The spectrometer for visible and near IR spectrum covers 400-1000 nm range with a band width of the channels of 5 nm. Optical instruments for short-wave IR range covers 900-2500 nm spectrum with a band width of the channels of 6.4 nm. Hyper-spectrometric data are recorded, compressed and subsequently processed by means of optical and digital tools. Calibration is performed before and after each spectrometric measurement to correct the data.

Fig. 3. Remote UltraCam device for a multi-channel video spectrometer

Different components, fabricated from optical polymers, are applied in the remote systems such as colour filters, scanning mirrors, protective windows, aspherical lenses for the imaging objectives, diffraction grating replicas, et al. Video data of the Earth surface is produced by the use of cameras for spectral photometry or hyperspectral systems [3-6]. For example, the unit Telops Hyper-Cam is the first spectral imaging camera [12]. It is a compact portable device with high resolution spectral imaging of Earth surface and atmosphere in land-, air-, and ecological applications. The

system may record images of cloud, luminance surfaces, geological and mineral formations, forest fires, pollution of water basins, volcano eruptions, military objects, etc.

The innovative optical instruments for hyperspectral remote measurements work in a broad spectral range from 400 nm to 14 μm and register images of distant objects. For satellite imaging cameras with 14-bit CCD detectors and format of 14000 x 9000 pixels are used. For example, the hyperspectral UltraCam device has 13 CCD detectors, among them 9 photo arrays create a wide panchromatic focal plane and the rest 4 matrixes ensure the red, green, blue and infrared channels (Fig. 3).

An optical aberration is a departure of the performance of an optical system from the predictions of paraxial optics [3, 17, 19]. Aberrations of optical systems are monochromatic and chromatic. Monochromatic aberrations are: spherical aberration, coma, astigmatism, field curvature and distortion. Spherical aberration is the only form of monochromatic axial aberration produced by rotationally symmetrical surfaces centered and orthogonal in regard to the optical axis. Spherical aberration will appear whenever the homocentricity of the incident optical beam is altered [17]. If all rays originating from the object, inclined by angle w in respect to the optical axis, are collected at one point in the plane of Gauss and this point does not coincide with the position of the image, this aberration is called distortion. Distortion is not affected by the relative aperture of the telescope objective but the radial displacement is proportional to the cube of the point field angle. In many of the astrophysical problems distortion does not influence the image quality. If for an infinitely distant object point, the optical system is free of distortion, it is called to be orthoscopic [3, 17].

Manufacturers of video spectrometers install and align the equipment according most stringent technical requirements, taking into account the field conditions of the environment. To achieve high optical performance with minimal weight of the imaging objective reflective schemes are used. In spectrophotometers concave holographic diffraction gratings are applied for aberration correction. The optical modulus is designed with an increased relative aperture at high image quality, aberrations are corrected and distortion of the objective is reduced in remote sensing systems [20, 21]

Refractometry of OPs ensures reliable determination of refractive and dispersive characteristics of polymer materials necessary for the spherochromatic correction in the design of optical systems [18, 22].

3. Characteristics of Optical Polymers

Application of OPs in the design of optical elements and systems is defined by their optical as well as mechanical and thermal characteristics. In aerospace instruments principal polymers as polycarbonate (PC), polymethyl methacrylate (PMMA), polystyrene (PS), methyl methacrylate styrene copolymer (NAS), as well as newer materials such as cyclic olefin copolymer (COC) and amorphous polyolefin (Zeonex) are used [5].

We have studied refraction, dispersion and transmission of over sixteen OPs, among them principal, as well as different trade-marks of polymer companies. Important optical parameters as refractive indices at the d-line (587.6 nm) n_d for VIS spectrum, as well as at s- (852.1 nm) n_s and t- (1013.9 nm) line n_t for the NIR band, Abbe numbers ν_d and ν_{879}, spectral transmission range *SR* have been measured or calculated [5, 18, 22]. Results of some of the studied OPs are presented in Table 1.

OPs are more sensitive to temperature environment conditions than optical glasses [18]. Contemporary optical devices with polymer components are designed in a large service temperature range from -40 °C to +60 °C. Among all OPs the PC material is with highest service temperature up to +130 °C and broadest operating temperature band -137°C÷130°C [18]. The Bayer polymer in Table 1 is a polycarbonate material too. Cyclic olefin copolymer, with a similar n_d as acrylic materials, provides a higher-temperature alternative. Its highest service temperature of 123°C is about 30°C higher than PMMA. Designers of polymer optics should be aware that environmental conditions should not exceed prescribed temperature requirements of the polymer producing companies. Another important parameter is the thermal expansion coefficient α_T of polymers which is with one order of magnitude greater than glasses. Refraction of OPs is also influenced by temperature and thermo-optical aberrations of polymer optical systems arise. Variations of refractive index of OPs with temperature $\Delta n/\Delta T$ are referred in literature as thermo-optic coefficients [22]. On base of our measurements in the temperature interval from 10 ^oC to 50 ^oC, the values of the thermo-optic coefficients have been calculated. Obtained results for $\Delta n_d/\Delta T$ and α_T from literature data [18] are included in Table 1. High-performance lens systems that require large temperature band operating conditions are more suited for hybrid glass-plastic design.

Mechanical properties of OPs are very important for their aerospace applications, too. High impact-resistance *I* is required (Table 1). The PC material with its extremely high *I* value is the most suitable polymer for

safety glasses, helmets and systems with long service durability. Another parameter for mechanical strength of OPs is their Young's tensile modulus *E*. Dynamic coefficients, obtained by means of our ultrasound measurements, are included in Table 1 and allow comparison with glass catalogue data [18]. Polymers have considerably lower density ρ which is from 2 to 4 times smaller in comparison to glasses. This is a great advantage of plastics which guarantees reduction of weight of the end optical systems. A ultra-lightweight, space-based telescope in geosynchronous orbit with a 20 m diameter, using polymer membrane optics and developed by Ball Aerospace & Technologies Corp has been reported recently [23]. This technology reduces the mass of large aperture telescopes by nearly an order of magnitude compared to those with conventional optics.

Table 1. Characteristics of optical polymers

	PC	PMMA	PS	Zeonex E48R	Optorez 1330	Bayer
n_d	1.5849	1.4914	1.5917	1.5309	1.5094	1.5857
n_s	1.5690	1.4837	1.5762	1.5228	1.5022	1.5705
n_t	1.5654	1.4819	1.5726	1.5209	1.4992	1.5669
ν_d	29.1	59.2	30.5	56.5	52.0	30.0
ν_{879}	54.6	96.7	56.4	100.5	71.7	54.3
$\Delta n_d/\Delta T$, $\times 10^{-4}$, K^{-1}	-1.00	-1.30	-1.31	-1.26	-1.20	-1.20
SR, nm	380÷1600	360÷1600	380÷1600	360÷1200	410÷?	380÷1600
$\alpha_T \times 10^{-5}$/°C	6.6÷7	5÷9	6÷8	6	7	6.5
I, J/m	600÷850	16÷32	19÷24	21	-	850
E, GPa	2.78÷3.37	4.17÷5.57	3.69	3.66	6.10	2.98÷3.53
$\rho \times 10^3$,kg/m^3	1.195	1.187	1.040	1.007	1.202	1.204

4. Analysis of the Thermo-optical Aberrations of Polymer Optical Systems

Calculation of geometric and wave aberrations is demanded to ensure image quality of optical elements. Residual monochromatic aberrations and chromatism distort processed information of analyzed objects. Influence of air temperature, humidity, pressure, etc. on image quality should be also regarded. Among common criteria of optoelectronic devices is determination of their point spread function and modulation transfer function. Transformation of light brightness at each point of the object surface into spatial frequency distribution of intensity in the image or

photonic sensor (CCD, etc.) plane is realized by a Fourier transform. Software programs on optical design calculate geometric and wave aberrations as well as point spread and modulation transfer functions if the material and design parameters are introduced as input data. However, the influence of environmental conditions is not considered. The aim of the optical design of systems with polymer or glass components is to ensure transfer of the object image to the detector with possible highest contrast and negligible distortion.

Temperature variations induce thermo-optical aberrations of polymer objectives which degrade image quality. The variety of available optical grade polymers is limited compared to that of glass and therefore possible combinations of OPs to create achromatic systems are restricted. The basic lens equation for its optical power Φ_λ is:

$$(1) \qquad \Phi_\lambda = 1/f'_\lambda = (n_\lambda - 1)(\rho_1 - \rho_2) + \rho_1 \rho_2 (n_\lambda - 1)^2 d/n_\lambda,$$

where n_λ is the index of refraction of the optical material at the d- standard wavelength λ_d or λ_e (546.1 nm), f'_λ – lens back focal length, $\rho_1 = 1/r_1$ and $\rho_2 = 1/r_2$ – curvatures and r_1 и r_2 – radii of curvature of spherical lens surfaces, d – lens thickness along the optical axis. Longitudinal chromatic aberration $\Delta s'_{FC}$ (axial separation between the red/blue F/C image distances) is:

$$(2) \qquad \Delta s'_{FC} = -f'_d / \nu_d,$$

where ν_d is the Abbe number at the d-line and F- and C- are the Fraunhofer lines with wavelengths $\lambda_F = 486.1$ nm and $\lambda_C = 656.3$ nm, respectively.

Differentiating of Eq. (1) with respect to n_d, we can determine the chromatic change of optical power $\Delta\Phi_d$ of a lens with thickness d as follows:

$$(3) \qquad \Delta\Phi_d = [(\rho_1 - \rho_2 + \rho_1 \rho_2 d (1 - 1/n_d^2)] \Delta n_{FC},$$

where $\Delta n_{FC} = n_F - n_C$ is the principal dispersion of the polymer material. When service temperature is changed the refractometric parameters as n_d, ν_d and Δn_{FC} are altered.

At a given n_d of the polymer material optimal lens design parameters r_1, r_2 and d are calculated to achromatize the position of its focal plane and achieve an achromatic lens. The chromatic change of focal length $\Delta f'_d$ is then calculated by means of Eq. (3):

$$(4) \qquad \Delta\Phi_d = F(\Delta n_{FC}) = \Delta f'_d / f'^2_d \quad \text{or} \quad \Delta f'_d = f'^2_d \Delta\Phi_d.$$

Achromatization of a single lens is difficult and therefore doublets and triplets are calculated to achieve minimal residual spherochromatism. When focal lengths at different wavelengths are equal $f'_F = f'_C$ and $\Delta\Phi_d = 0$ but $f'_d \neq f'_F$, residual chromatism exists and the spherochromatism is determined by the difference of spherical aberrations $\Delta S'_F - \Delta S'_C \neq 0$.

The refractive index n_T of optical material at a given temperature T in °C is determined by the expression:

(5) $$n_T = n_\lambda + \beta_{T,\lambda}\,(T - 20°),$$

where n_λ is the catalogue refractive index at a given wavelength λ, measured at temperature of 20 or 22 ºC according to the European or USA standard and $\beta_{T,\lambda} = \Delta n_\lambda / \Delta T$ is the thermo-optic coefficient at a certain wavelength λ.

Denoting the thermo-optic constant $V_{T,\lambda} = [\beta_{T,\lambda} /(n_\lambda - 1)] - \alpha_m$, we get:

(6) $$n_T = n_\lambda + [(n_\lambda - 1)\,(V_{T,\lambda} - \alpha_T)]\;T / n_\lambda,$$

where α_T is the thermal expansion coefficient of the material or the relative elongation of the polymer sample at measured temperature T and α_m is the mean coefficient in the temperature interval from –60 °C to +20 °C or from +20 °C to +120 °C [17, 18].

For optical materials the thermo-optic constant $V_{T,\lambda}$ characterizes the change in refractive index and dispersion of the refractive element with temperature. The values of $\beta_{T,\lambda}$ and $V_{T,\lambda}$ are standardized and are presented in optical database for glasses, plastics, ceramics, nano-composites, etc.

Temperature change of refractive index Δn_T in respect to n_λ at standard temperatures:

(7) $$\Delta n_T = n_T - n_\lambda,$$

can be used to analyse the thermo-optical aberrations in the design of optical systems [18]. For principal OPs, on base of our measurements, $\Delta n_T \times 10^{-4}$ °C for the d-line is: 9.0 (PMMA), 13.0 (PS) and 5.0 (PC) in the temperature interval between 10 and 20 °C; and 39 (PMMA), 39.3 (PS) and 30 (PC) in the range (20 ÷ 50) °C.

In case of an achromatic system (Fig. 4a) with two PC mirrors, mirrored surfaces undergo thermal linear expansion but Δn_T of the PC material doesn't change their optical power. The mirror focal length f'_m is determined only by its radius of surface curvature r_m as follows [3, 17]:

(8) $$f'_m = r_m/2 \quad \text{и} \quad \Delta f'_T = 0.5\, r_m\, T\, \alpha_T,$$

where $\Delta f'_T$ is the temperature change (the thermo-optical aberration) of focal length which is calculated by means of Eqs. (1) and (4).

A spherical mirror has about eight times smaller spherical aberration in comparison to an analogues plano-convex lens and [3]:

(9) $\Delta S'_m = -0{,}25\ \rho_m\ h^2,$

where h is the height of the incident ray ($h_{max} = D/2$), D is the mirror diameter and $\rho_m = 1/r_m$ is the curvature of the mirrored optical surface.

The optical power Φ_m of the two-component mirror system (Fig. 4a) is calculated according the expression:

(10) $\Phi_m = 1/f'_m = -(\Phi_1 + \Phi_2 + \Phi_1\ \Phi_2\ d),$

where d is the separation distance between the components along the optic axis, f'_m is the focal length of the mirror system, Φ_1 and Φ_2 represent the optical power of the two spherical mirrors. Temperature alternation of the optical power $\Delta\Phi_T$ is determined by differentiating of Eq. (10) taking into account variations of mirror focal lengths $\Delta f'_{m_1}$ and $\Delta f'_{m_2}$ caused by thermal changes of the mirror radii Δr_{1T} and Δr_{2T}:

(11) $\Delta\Phi_T = \Delta f'_T / f_m^{\,2} = -(\Delta\Phi_{1T} + \Delta\Phi_{2T} + \Phi_1\ \Phi_2\ \Delta d_T),$

where $\Delta\Phi_{1T}$ and $\Delta\Phi_{2T}$ are variations of the optical power of components. Small values of second order are neglected but for the temperature interval $\Delta T = 40°$ (from –10 °C to +30 °C) the $\Delta\Phi_T$ value is significant.

The optical power of a plano-convex lens is calculated as follows [3]:

(12) $\Phi = 1/f' = (n_d - 1)/r$ or $r = (n_d - 1)\ f',$

where r is radius of the convex surface curvature and f' is the lens focal length.

Differentiation of Eq. (12) in respect to temperature change of the lens back focal length f' gives:

(13) $\Delta f'_T = (\Delta r_T - f'\ \Delta n_T)\ /\ (n_d - 1),$

where Δr_T is calculated by the relation $\Delta r_T = r\ T\ \alpha_T$ for the temperature interval from –10 °C to +30 °C. Spherical aberration of the plano-convex lens is determined by [3]:

(14) $\Delta S' = -0{,}5\ (n_d\ h^2)\ /\ (n_d - 1)\ r,$

where $h = D/2$ is the lens aperture diameter.

The size of the image Y' at the back focal plane of the imaging objective is determined by the relation [3, 17]:

(15) $Y' = f' \operatorname{tg} \omega,$

where ω is the objective field of view. Temperature change of the image size is calculated by:

(16) $\Delta Y'_T = \Delta f'_T \operatorname{tg} \omega ,$

where $\Delta f'_T$ is determined by Eq. (13).

For an achromatic objective the temperature optical power change of first order is calculated by the relation:

(17) $\Phi_1 / \nu_1 + \Phi_2 / \nu_2 = 0 \; ; \; \Delta\Phi_{1,T} = -(\nu_1 / \nu_2)\, \Delta\Phi_{2,T},$

where Φ_1 and Φ_2 represent optical power of the positive and negative lens and ν_1 and ν_2 – Abbe numbers of OPs at the standard wavelength λ_d. Alterations $\Delta\Phi_{1,T}$ and $\Delta\Phi_{2,T}$ are calculated by consecutively differentiating of Eq. (1) in respect to Δn_T, Δr_T and Δd_T for each of the lenses. On the base of the partial dispersion formula [18] the temperature change of first order of the Abbe number is determined as:

(18) $\Delta\nu_{d,T} = (\nu_d\, \Delta n_{d,T}) / (n_d - 1),$

where n_d and ν_d is the refractive index and Abbe number of the applied polymer, respectively and $\Delta n_{d,T}$ is calculated by means of Eq. (7). Lateral chromatism is obtained on base of Eq. (15) as:

(19) $\Delta Y'_{FC} = Y'_F - Y'_C,$

where Y'_F and Y'_C are the image sizes created by the positive system (lens, achromat or triplet) at standard wavelengths λ_F and λ_C. The chromatic image error $\Delta Y'_{FC}$ depends on principal dispersion of OPs $\Delta n_{FC} = n_F - n_C = (n_d - 1) / \nu_d$.

5. Lens Design for a Remote Sensing Device

Spectrometric systems Spectrum-15 and Spectrum-256, intended for RS of Earth, were used during the flights of the Bulgarian astronauts G. Ivanov and A. Aleksandrov. Presented design of the aberration compensators for the objective, used in the video spectrometers, is based on the theory of optical systems [3, 17]. Objectives with excellent optical characteristics and aberration correction in the full field of view are required

for remote sensing spectrometers. Decrease of distortion is necessary for the optical schemes of cameras with CCD arrays [20, 21]. Coma, which is the second odd aberration, is difficult to be eliminated in case of systems with a limited number of components. OSLO optics software has been used for the study of properties of the synthesized objective with two aberration compensators. Analysis of the wave aberrations as well as of the point spread function is required to determine the energy distribution in the Airy's diffraction pattern [21].

The modular approach for the synthesis of complex optical systems is very flexible and convenient for objectives used in various applications of instrument engineering and optoelectronic devices [3, 17]. Odd aberrations as meridional coma and distortion are difficult to be eliminated in the full field of view of the objectives. The influence of the meridional coma is analysed by relating comatic circles' radii with all of the design parameters of the afocal double lens compensator [3]. The modular approach consists in attaching of two lens compensators to the Cassegrain objective, which is comprised of two basic mirrors, in order to achieve a separate correction of the meridional coma and distortion (Fig. 4b).

A method for aberration correction of the considered mirror-lens objective is proposed. If the design parameters of the optical system are assumed as back focal length $f' = 500$ mm, relative aperture $D/f' = 1{:}5$ and field of view $2\omega = 3.4^{\circ}$, and it consists of two permanent polycarbonate spherical mirrors and two varying quartz aberration compensators located close to the mirrors, the aberration compensation is realized by: a) the first afocal compensator for correction of spherical aberration and meridional coma (Fig. 4a); b) second compensator, located next to the primary mirror, to reduce field aberrations as astigmatism and distortion (Fig. 4b); c) relative motion of the first compensator away from the convex mirror to reduce vignetting of obliquely incident rays (Fig. 5); d) relative motion of the second compensator away from the concave mirror to improve aberration correction but reduces field of view (Fig. 5); e) diffraction at entrance pupil of the objective doesn't restrict its resolution ability (RA) and the meridional coma is the most significant residual aberration (Fig. 4b and d).

The image quality of the proposed optical system is verified on base of calculated modulation transfer function (Fig. 4c) and point spread function (Fig. 4d). Two modifications of the mirror-lens objective are

investigated: 50 % vignetting of the obliquely incident rays and without ray vignetting at the end of the field of view [21].

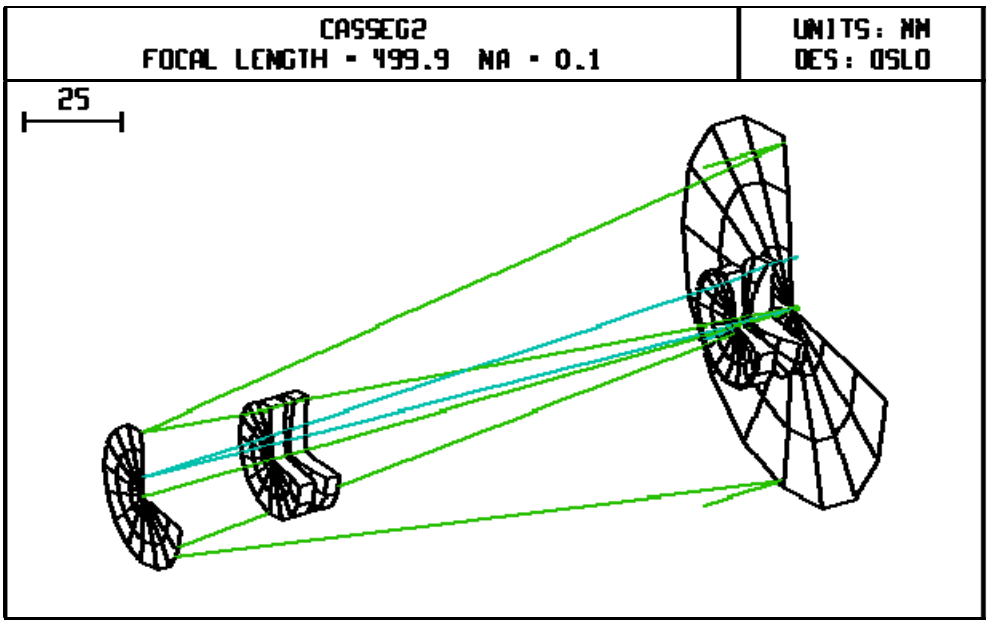

a)

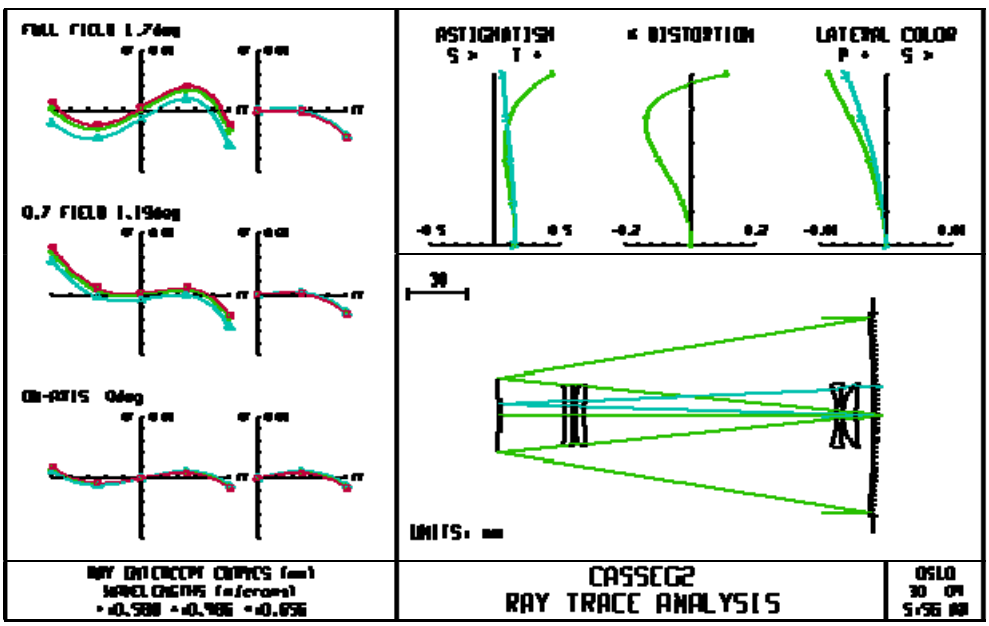

b)

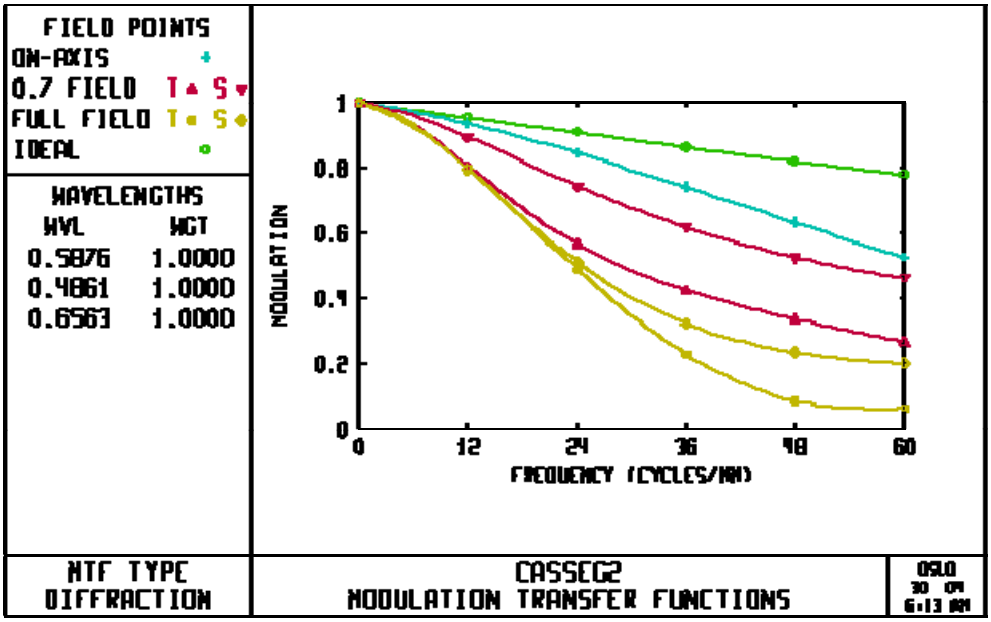

c)

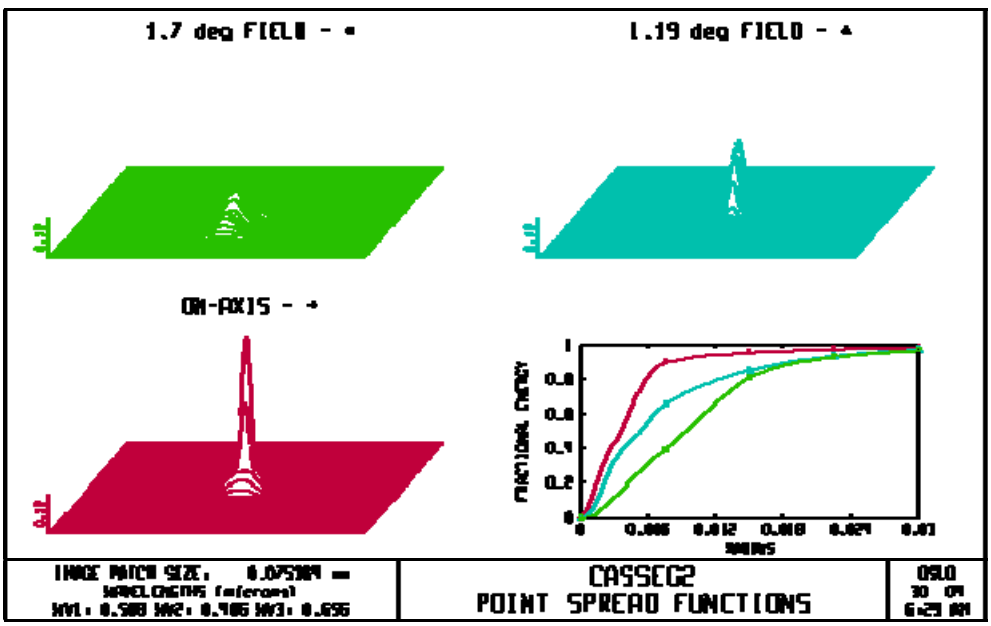

d)

Fig. 4. Remote imaging mirror-lens system with two aberration compensators: (a) a 3D design of the objective; (b) geometric aberrations and ray trace analysis; (c) modulation transfer function;(d) point spread functions

The design of the final hybrid objective with on-axis and oblique ray tracing is presented in Fig. 5. Mirrors are made of polycarbonate shells mirrored with aluminum coatings and protected with anti-abrasive layers to minimize the size and weight of the objective in the remote sensing spectrometer. Field aberrations are reduced to a spot size bellow 0.013 mm. The achieved aberration point spread spot is significantly smaller than the CCD pixel (0.016 x 0.016 mm or 0.024 x 0.024 mm). The modulation transfer function of the obtained objective reaches spatial frequencies of 40 lin/mm (Fig. 4c) and meets the requirements of the video-spectrometric modulus [3, 20, 21].

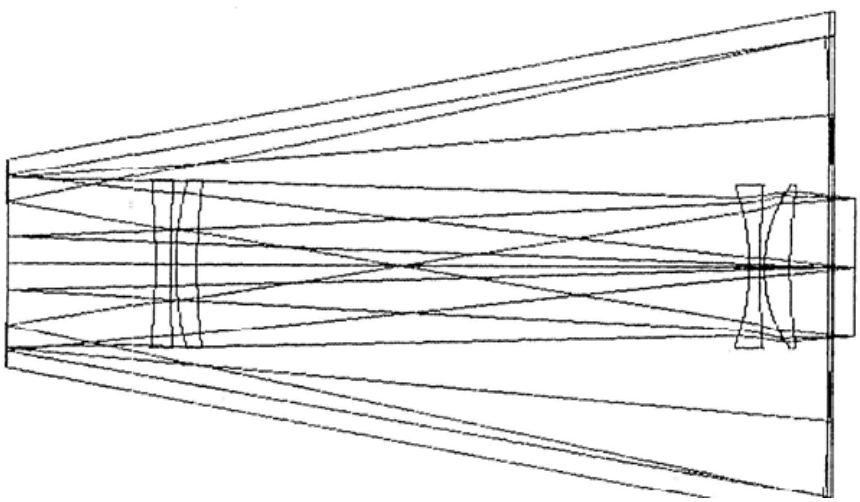

Fig. 5. Final design of remote imaging mirror-lens objective with on-axis and oblique ray tracing

6. Applications of Optical Polymers in Remote Imaging Systems

Vision plays a crucial role in life and labor activity of people [3, 4, 24]. Up to 86-90% of the information about the world is perceived by eyes and then transferred to the brain. Optical methods facilitate physicians in the diagnosis of vision and establishment of the state of health of people applying for various professional positions (drivers, pilots, police officers, etc.). Information abilities of vision reach 10^{12} bits (bio-computer) at about 14 Hz clock frequency of brain during stereoscopic observation of coloured objects, which is comparable to the volume of known terabyte optical memories [4, 25, 28]. The eyes function in a huge dynamic range from 10^{-7}

cd/m² to 10^5 cd/m² during light/dark adaptation as RA and visual contrast sensitivity constantly change. Cinema / TV transmissions are performed at a frequency of 24/25 fps at information volume of the images around 10^6 bits. The human eye has a momentum approximately 0.1s perception of light images in which the critical frequency of vision is 16-25 Hz for watching cinema / TV movies [24, 29]. The spaceman vision reality is given in [4]. The eye's contrast sensitivity is evaluated as 1 – 2%. The speed of the visual reactions of pilots reaches 0.05 - 0.025s and they operate at critical frequencies up to 50-60 Hz. High visual facilities of astronauts, pilots, and operators of high-speed machines are certified by measuring methods of ophthalmology. For aerospace staff the visual requirements demand stereoscopic RA to 3-5", linear RA of at least 0.05 mm at the plane of the measuring scale, and sustainable observation of the control panels of the monitoring devices of about 3 to 5 min. In Fig. 6 aerospace helmet displays for remote connection with the pilots in flight are presented. Frontal transparent helmet modules for stereoscopic display are made of PC polymer material, which has the highest impact strength (Table 1). Binocular display is assembled with different optical polymer systems: magnifiers, VIS or NIR goggles, viewfinders, measuring screens, etc. Work surfaces of the PC front module displays of helmets are covered with anti-reflective, hydrophobic anti-abrasive optical layers.

a) b)

Fig. 6. Helmet displays for remote aerospace systems: a) Binocular Display improves pilots' eyesight options for target designation; b) Helmet Display system increases the accuracy of pilots's measurements

"One picture is worth a thousand words": physicians recognize the tissues of living organs using qualitative color medical images. A swallowable capsule camera made from optical polymers can transmit up to 50 000 color pictures for the digestive tract of the pilot [26, 27]. A remote medical control can be fulfilled when the patient swallows the camera with a size of a drug capsule, which moves smoothly and painlessly through the esophagus tract by means of peristalsis (Fig. 7). Traveling in the living body, the capsule transmits video signals received by an antenna located outside the body of the respondent. Photos are saved in a wireless device installed in the belt of the pilot. Through Internet line doctors supply recorded medical data in a computer station that is equipped with software for processing of optical images. A short video movie with information about the pilot's digestive tract during the remote examination is obtained. The capsule camera, shown in Fig. 7, represents a remote imaging tool: the patient with it is far away from the medical command center (in flight, at work, on a business trip, on the road, etc.). The polymer video capsule is removed from the body in the natural way, i.e. it is a disposable optical device. The respondent doctor at the diagnostic center receives the recorded images of the esophageal tract and remotely connects and consults the patient by means of telecommunication equipment (video mobile phones, optical Internet networks, etc.).

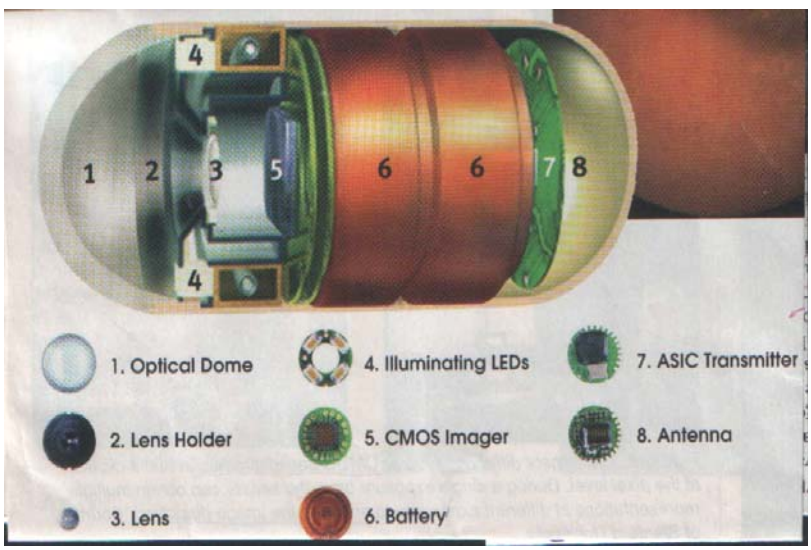

Fig. 7. A polymer swallowable capsule camera for remote diagnostics of aircraft's digestive tract (Tufts University School of Medicine, Boston, MA)

The optical dome (1) in Fig. 7 and the cylindrical body of the disposable capsule are produced from a bio-inert full-polymerized PMMA material. The endoscopic objective (3) is assembled from PMMA and PS lenses designed for a good spherical and chromatic correction over the image field [5, 18]. The frontal surface of the optical dome (1) is sputtered with anti-reflexive and anti-acid coatings.

OPs have a broad range of applications: single lenses and lens arrays, assembled components, aspheric polymer layers deposited on glass lenses, metal-ceramic mirrors with protective polymer coatings, mirror optical systems, integrated optoelectronic modules, etc. [5, 18]. In recent years polymer optoelectronics is introduced: nanocomposite materials with a negative refractive index, polymer pads with arranged metal atoms, surface diffraction films and plasmon structures, one-dimensional arrays of micro-lenses for coupling of micro-lasers with vertical cavity for fiber optic communication modules, two-dimensional nano-focusing arrays for recording and reading data from terabyte memories, OP matrices with arranged magnetic dipoles, nano-and micro-magnets, magnetic heads, etc.. [18, 25].

7. Summary and Conclusions

Polymer materials are widely applied in science and technology, optoelectronics, aerospace, defense industry, etc. Optical, mechanical and thermal characteristics of OPs are pointed out. The design and aberration analysis of a mirror-lens objective based on the Cassegrain optical scheme, used in video spectrometers for remote sensing, is proposed. Formulae for thermo-optical aberrations of polymer optics are derived. Geometrical and physical optics form the theoretical bases of the hyperspectral measurements which are intended for colour imaging and monitoring of global surfaces. A SITe 1100 x 330 Scientific-Grade CCD sensor with imaging area of 26.4 x 7.92 mm and pixel size 0.024 x 0.024 mm with high quantum efficiency from the UV to NIR spectral region (280 ÷ 1100 nm) has been proposed. The optical module of the imaging spectrometer works at 200 mm aperture diameter and focal length of 500 mm with good aberration correction of the objective. The optimized scheme is compact and the objective is with small longitudinal dimensions and limited central vignetting for location of the image behind the principal mirror (Fig. 5). The linear dimension of the imaging field is 30.7 mm and the maximal diameter of the aberration spot is

0.013 mm in the VIS spectrum which is twice smaller than the given pixel size of the CCD imaging array (Fig. 4).

The new applications of OPs are designs of hybrid and nano-composite devices used in aircraft and communication networks. The innovative robotic and adaptive stations are under research and development, intended for generation and remote transmission of million colour and spectral-zonal images of the Earth surface. The new OPs are applied in nano-photonics for the design and fabrication of nano-scale components, information systems for image processing, micro- and helmet-displays, nano-computers, etc. The doctors are responsible to examine the parameters of eyesight and digestive tract of pilots before every flight. The binocular and helmet displays secure a remote vision control of aviators in flight using transmitting/receiving images from/to the aerospace center. A swallowable polymer camera is presented for remote biomedical testing of the spaceman stomach with intestines. Our research is directed to the analysis and synthesis of nanocomposite OPs applied for the realization of hybrid optoelectronic devices that can be used in remote stations for recording of ecological catastrophes and hyper-spectral pictures.

References

1. Космическая оптика.- Пер. с англ., изд. „Мир", Москва, 1985.
2. М и ш е в, Д. Дистанционни изследвания на Земята от Космоса. изд. на БАН, София, 1981, 206 с.
3. Н и к о л о в, И. Оптични методи и системи (за запис и обработка на информация). Унив. изд. „Св. Климинт Охридски", София, 1993, 272 с.
4. М а р д и р о с я н, Г. Природни екокатастрофи и тяхното дистанционно аерокосмическо изучаване. Акад. изд. „Проф. Марин Дринов", София, 2000, 387 с.
5. N i k o l o v, I., N. S u l t a n o v a, S. K a s a r o v a, Polymer materials for NIR and laser applications, SES 2013, 9th Sc. Conf. with Int. Part. "Space, ecology, safety", 20-22 Nov 2013, Sofia, Bulgaria: (to be published).
6. M a r m o, J. Hyperspectral imager will view many colors of Earth. Laser Focus World, August 1996, pp. 85-91.
7. S c h o t t, J. Spectral data adds a new dimension to remote imaging of Earth. Laser Focus World, August 2004, pp. 76-84.
8. C o s i m o, J. C., C. L. P a r k i n s o n. Satellite-Observed Changes in the Arctic. Physics Today, August 2004, pp. 38-44.
9. J o n e s-B a y, H. A. Hyperspectral imagers shed light on pharmaceutical processing methods. Laser Focus World, December 2004, pp. 95-98.

10. F l a n d e r s, D. R., A. H. M e n g e l, B. S. T e r r y. Remote Sensing Applications in Regional Emergency Management. PHOTONICS SPECTRA, March 2006, pp. 70-76.
11. H o g a n, H. Satellite Imagery Comes Down to Earth. PHOTONICS SPECTRA, August 2006, pp. 48-54.
12. www.telops.com (Telops Inc., Quebec, Canada).
13. B a n n o n, D., R. T h o m a s. Harsh environments dictate design of imaging spectrometer. LaserFocus World, August 2005, pp. 93-97.
14. W e t h e r i l l, G., A. A l r e e, K. B u r k e (Editors). Annual Review of Earth and Planetary Sciences.1991, pp. 351-382.
15. M i c h e v, D. Spectral Characteristics of Natural Formations. BAS Publishers, Sofia, 1986.
16. М и х е л ь с о н, Н.Н. Оптические телескопы (теория и конструкция).- Наука, Москва, 1976.
17. Р у с и н о в, М.М. Техническая оптика.- Машиностроение, Ленинград, 1979, 488 с.
18. С у л т а н о в а, Н., С. К а с ъ р о в а, И. Н и к о л о в. Рефрактометрия на оптични полимери (под об. ред. на проф. И. Николов), Унив. Издат. „Проф. д-р Асен Златаров“, Бургас, 2013, 176 с.
19. S m i t h, W. J. Modern Lens Design.- “McGraw Hill”, New York, 1992.
20. N i k o l o v, I., Z. Z a h a r i e v a. Mirror-lens Optical System for Image Spectroscopy Device. Proc. of SPIE, Vol. 3573, 1998, pp. 413-416.
21. N i k o l o v, I., A. K r u m o v, Z. Z a h a r i e v a. Optical Lens Assembly for Image Spectrometry. “Physics Letters”, № 11, 2000 (BPU-4, 22-25 August 2000, Veliko Turnovo).
22. N. G. S u l t a n o v a, S. N. K a s a r o v a a, I. D. N i k o l o v, Characterization of optical properties of optical polymers, Optical and Quantum Electronics, Vol. 45, no. 3, 2013, pp. 221- 232.
23. www.photonics.com, Membrane Optics Telescope Demo’d for DARPA, Dec. 9, 2013.
24. M a r r, D. Vision. W. H. Freeman and Company, New York, 1982, 400 p.
25. N i k o l o v, I., K. K u r i h a r a, K. G o t o. Nanofocusing Probe Optimization in a Near-Field Head for an Ultra-High Density Optical Memory. Chapter 2 in Focus on Nanotechnology Research, Ed. Eugene V. Dirote, Nova Science Publishers, Inc., New York, 2004, pp. 19-49.
26. P o w e l l, P. M. Maximizing Output with Miniature Cameras. Photonics Spectra, July 2002, pp. 46 – 52.
27. H i n d u s, L. A. Medical Imaging Patients Find Easy to Swallow (Swallowable Endoscopy Capsules). ADVANCED IMAGING EUROPE, October 2002, pp. 18-21.
28. К а л и м а н о в а, И., И. Н и к о л о в. Светлинни измервания. Глава 12 в Метрология и измервателна техника под об. ред. на проф. Х. Радев, Софттрейд, София, том 3, стр. 351 - 482.
29. Б а р а б а н щ и к о в, В. А. Динамика зрительного восприятия. Наука, Москва, 1990, 239 с.

НЯКОИ АЕРОКОСМИЧЕСКИ ПРИЛОЖЕНИЯ НА ОПТИЧНИТЕ ПОЛИМЕРИ

И. Николов, С. Касърова, Н. Султанова

Резюме

Оптичните полимери (ОП) намират широко приложение в оптоелектронните уреди и системи, предназначени за дистанционна образна диагностика на земната повърхност. Дадени са експериментални резултати за някои оптични, механични и топлинни характеристики на основни ОП. Предложен е дизайн на огледално-лещов обектив по схемата на Касегрен, включващ две базови поликарбонатни огледала и два променящи се кварцови аберационни компенсатора. Изчислени са геометричните и вълнови аберации. Обективът е подходящ за работа на видео-спектрометрите за дистанционни изследвания. Представен е анализ на индуцираните термо-оптични аберации на полимерни оптични системи. Илюстрирано е използването на полимерните материали за дистанционно диагностициране на зрението и общото здравословно състояние на авиационния състав посредством поглъщаема капсулна камера за еднократна употреба, фронтални модули на бинокулярни шлемови дисплеи и други съвременни приложения на ОП.